Ultra-stable Transformer Oil nanofluids with significant AC Breakdown Voltage enhancement at ultra-low filler fraction of functionalized boron nitride nanosheets

Mississippi Missouri Bhunia[1], Kalyan Kumar Chattopadhyay[2*], Paramita Chattopadhay[1*]

[1]*Department of Electrical Engineering, Indian Institute of Engineering Science and Technology, Shibpur, Howrah-711103, India*

[2]*Department of Physics, Jadavpur University, Kolkata-700032, India*

*Corresponding author:

email address: kalyan_chattopadhyay@yahoo.com, paramita_chattopadhyay@yahoo.com

phone: 923164811, 9433389445

ABSTRACT

This paper reports the purposeful fluorination of hexagonal boron nitride (h-BN) nanofillers and its impact on reinforcement of AC breakdown strength and stability of transformer oil (TO) nanofluid. Fluorine functionalized boron nitride nanosheets (f-BNNs) of ~5 nm thickness was synthesized in house via wet synthetic exfoliation route of pristine h-BN utilizing Ammonium Fluoride (NH_4F) as the shedding agent. This promotes attachment of some highly electro-negative fluorine atoms to boron. This tailored f-BNNs exhibit a diminished band gap and induced electrical conductivity which helps in elevating the AC breakdown Voltage to 26 %-20% and a surge in resistivity at appreciably low nanofiller fraction of 0.005-0.01wt. %. These noteworthy improvement of electrical insulation properties compared to the state-of-the-art Boron nitride nanoparticles or nanosheets is explained by the parallel role played by fluorine in charge trapping as well as the role played 2D morphology of the nanofillers. Here, fluorine facilitated extrinsic energy bands in the oil-nanofiller interface acted as efficient charge trapping sites and helped to accumulate large quantities of streamer charges, more than h-BN nanosheets or BN nanoparticle for a longer time and improved the electric insulation properties to a large extent. The ultra-high steadiness of the nanofluid is also observed at these lower filler concentrations. 2D morphology, lipophilicity and electro-negativity induced electrostatic repulsion between the f-BNNs nanosheets are attributed to achieve this alluring property of the nanofluid. Such significant improvements at very low filler fractions justifies the fluorination of hexagonal boron nitride as a novel idea and a better alternative among all the reported BN brothers for high voltage applications of nano engineered liquid insulation.

Keywords: Fluorine functionalization, f-BNNs, AC Breakdown, Electronegativity, stability

1. Introduction

Since their advent by Choi in 1995 [1], nanofluids have played extensive role in advanced cooling systems such as electronic industry, automobile sector to nuclear power plants [2] and etc. In the electrical power industry, the concept of nanofluids was introduced primarily to improve the electrical properties (dielectric breakdown strength, impulse breakdown voltage, PDIV, etc.) of insulating fluids (mineral oil, transformer oil & alternatives) so that the rising problems of liquid insulation failures could be taken good care of. The registration of the research on nanodielectric fluids can be dated back to the work of Segal *et. al*. [3] where magnetic nanoparticles (spherical, Fe_3O_4) were used for the aim of improvement of dielectric breakdown (DB) properties of mineral oil. It was seen that the dielectric breakdown strength (DBS) of mineral oil was dependent on external magnetic field direction [3]. Later, several non-magnetic nanoparticles such as TiO_2, SiO_2, Al_2O_3, BN & etc gained their due importance in this field [4-7]. In the last decade, along with electrical insulation, the idea of dielectric nanofluids was extended towards improving the cooling performance of insulating fluids [8]. Parallelly, research using some alternative oils as base oil such as ester/ vegetable oils were conducted due to poor biodegradability of mineral oil [9].

The mechanism of electrical breakdown is extremely complicated. It depends upon various parameters of base fluid (moisture content, viscosity, temperature) [10], measurement protocols [11], purity [12] etc. Electrical breakdown in nanofluid is a surface phenomenon [4]. The oil-nanomaterial interface plays a huge role in enhancing BDV by acting as a scavenger of streamer charges [4]. Hence, in nanofluids, apart from the previously mentioned factors, properties of the nanofiller such as conductivity, permittivity, morphology, size of nanofiller own their respective influences. For example, Mohammad *et al.* [13] compared the AC BDV and viscosity of natural ester oil based three types of nanofluids. The ester oil-based nanofluids were prepared by mixing palm fatty acid ester (PFAE) oil with three types of nanoparticles (conducting Fe_3O_4, semi-conducting TiO_2 and insulating Al_2O_3) of size,15-20 nm at a concentration of 0.01 g/L The ferrofluid was the best to show a 43 % improvement in AC BDV. Similarly, Wenxia Sima *et al.* [14] studied the relative performances of conducting Fe_3O_4, semiconducting TiO_2, and insulating Al_2O_3 nanoparticles with *size*,10 (± 0.1) nm, modified by Oleic acid, Stearic acid and Span 80 in TO. Due to the differences in the conductivity and the dielectric constant, the rate of electron scavenging at the interface was found to be different for different material. This led to different degree of improvement in impulse BDV. Fe_3O_4, TiO_2& Al_2O_3 showed almost 44, 33 & 35 % increase in impulse BDV at 0.003, 0.006 &0.006 Wt. %

respectively. Hence, in the context of conductivity and permittivity, high conductive & low relaxation time of the conducting nano fillers enhance the breakdown properties to a large extent at ultra-low concentrations [15]. In line with this, some of the recent studies with ultra-high conducting fillers such as CNT, graphene [15] have been reported. On the other hand, semi-conducting [16, 17] and insulating [18] fillers require moderate to high filler fraction to achieve the same performances. At relatively higher filler fraction, due to large attractive van der Waals forces among nanomaterials, the agglomeration accelerates and the long-term stability of the NFs are questionable. Many researchers have demonstrated that stability of NFs using of surfactants like oleic acid have been enhanced due to static hindrance [19]. But long-term functionality of these long chain molecule are doubtful, as loosely surrounds over the fillers [19, 14]. Moreover, these surfactants are corrosive in nature and not suitable candidate for transformer core.

On the other hand, morphology of the nanofillers also play a significant role to improve the charge trapping capacity and other thermo physical properties [17]. Hence, search for customized nanofillers is the need of the hour to address the issues of insulating and thermal properties along with long-term stability of the NFs. Recent development of two-dimensional (2D) layered materials presents a unique opportunity to address several of the aforementioned problems. Properties of these 2D materials range from metallic (NbS_2, VSe_2), conducting (graphene), semi-metallic (WTe_2, $TiSe_2$), semiconducting (MoS_2, WS_2) to insulating (h-BN, HfS_2); and their properties can even be tailored to suit specific base fluids [20]. Owing to their 2D nature, these nanofillers have extremely high surface to volume ratio and thus can be operated at much lower filler fractions to obtain targeted outcomes. The layered structure gives ultra-thinness to these materials so that they are easily stable in the base fluids [20, 21]. Hence, a proper tailor made 2D nanomaterial would lead to design an application specific nanofluid. Among many 2D nanomaterials, h-BN is highly insulating with outstanding thermal conductivity, first-rate mechanical steadiness, and prominent chemical dullness. Du *et al*. [7] demonstrated that BN nanoparticle improves thermal responses, electrical insulation and BDV of TO. However, BN particles tend to agglomerate easily [7]. Later, Bhunia *et al* [8] &Tijerina *et al* [21] pointed out that chemically exfoliated h-BN nanosheets, owing to their 2D structure and ultra-thinness with large surface exposal of (002) planes can be a better choice for designing next-generation TO NFs. As an extension to the previous study on h-BN nanosheets as well as recalling he extraordinary performances of conducting nanofillers at ultralow concentrations [15], the present work is a novel approach to explore the effect of a tailor made, 2D conducting nanofiller in TO. Conducting and

electro-negative fluorine functionalized h-BN nanosheets called fluorinated boron nitride nanosheets (f-BNNs) has been picked up for this purpose. Novelty of the investigation lies on the intended fluorination of h-BN Nanosheets for band engineering to achieve elevated AC breakdown voltage at very low filler fraction as compared to h-BN. Eventually the diluted filler fraction and electro-negativity of the functionalised material has improved the stability of the TO NF to a great extent.

The following sections discusses the methods employed and the experiments performed. The outcomes of the results are discussed elaborately with suitable references. Schematics are used to discuss the mechanisms involved.

2. Materials and Method

2.1 Synthesis

All the required chemicals were bought from Sigma Aldrich and were used without further purification. Ammonium Fluoride (NH_4F) and bulk hexagonal boron nitride (h-BN) powder (~1 µm) were taken in certain proportions in a mortar and pestle (in 5:1 ratio) and grounded to homogeneous form. Next, 20 mL distilled water (DI) was added to it and mixed thoroughly. The solution was afterwards transferred to Teflon lined stainless steel autoclave and then heated at 180°C for 24 h. After natural cooling down, the resultant product was washed with DI until the pH reduced to neutral. Thereafter, the sample was dried in a petri dish at 80°C for 24 h in a preheated oven. Finally, white powder of f-BNNs was collected and stored for further characterization.

The formation of f-BNNs from commercial BN is achieved by fluorinated cum exfoliated route. The consumed mediator for exfoliation, i.e., NH_4F breaks up into F^- and $NH4^+$ ions. Now, F^- being highly electro-negative and reactive, causes some B atoms of BN to come out of its basal planes disturbing the regular SP^2 configuration of BN. This causes edge buckling in bulk h-BN and results in successful scrolling of individual sheets to reduce surface tension. The edge scrolling enables the diffusion and intercalation of $NH4^+$ ions. $NH4^+$ ions having relatively larger size than inter planer space can increase the distance between h-BN stacks with a motion perpendicular to the BN plane with high mobility. The resultant mechanism results in exfoliation and fluorination of few layers h-BN sheets. The mechanism is schematically expressed in **Fig. 1a**.

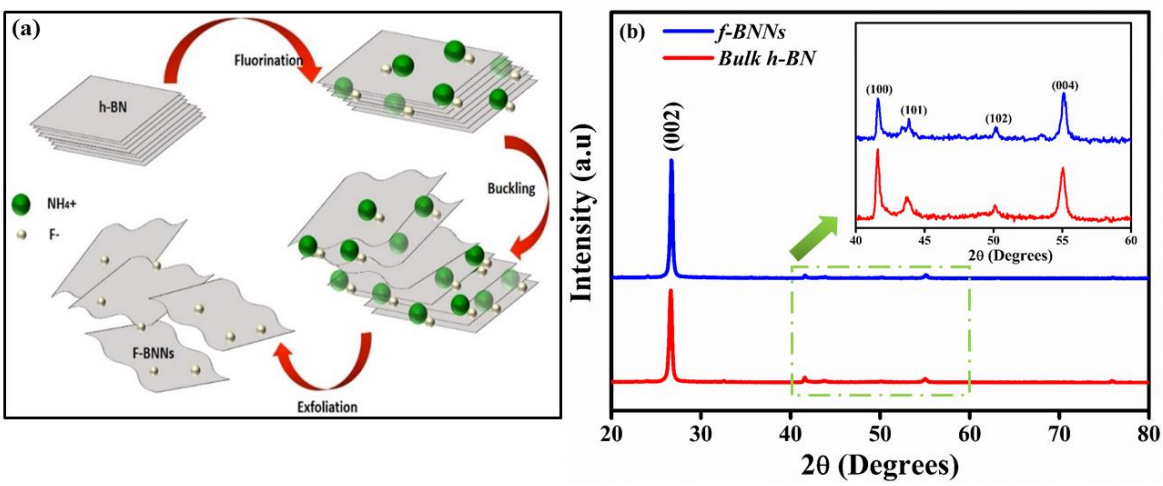

Fig. 1 (a) Step by step exfoliation route & (b) XRD of f-BNNs

2.2 Characterization and Experimentation

The phase purity of the synthesized samples was studied by recording X-ray diffraction (XRD) pattern (via *Bruker D-8 Advance Diffractometer, operating at 40 kV, 40 mA*) using Cu-Kα radiation (λ=1.54 A). Characterization and identification of the functional groups were performed by *Shimadzu IR PRESTIGE 21* spectrometer within the range of 500-4000 cm^{-1}. Raman spectra of the synthesized samples were recorded by *WI Tec Raman spectrometer, Nd:* YAG laser with an excitation wavelength of 532 nm. The samples were further characterized by high resolution transmission electron microscope (HRTEM), *JEOL 2100 (Operating voltage: 200 kV)* and Field emission Scanning Electron Microscope (FESEM), *ZEISS* for determining its nanostructures. The Energy Dispersive X-Ray Analysis (EDAX)was carried out (in the FESEM machine) for compositional study of the material. X-Ray Photo Electron Spectroscopy (XPS) analysis (using monochromatic Al Kα (*hν* = 1486.6 eV) as X-ray source and a hemispherical analyser (SPECS, HSA 3500)) was conducted to identify the chemical states. Tests of AC breakdown voltages of the f-BNNs-Transformer oil nanofluids were carried out using Neo-Tele-Tronix made 120 kV, 50 Hz automatic breakdown voltage testing equipment. The Tan Delta and Resistivity of the nanofluids were measured by *ADTR 2K Plus* instrument, supplied by ELTEL industries. The temperature dependent thermal conductivity of nanofluids at various filler fractions were carried out by KD2 probe thermal Property analyser (*Decagon Device Inc*., model *KD2 Pro, KS1* probe for liquids) following a lab set up similar to [22]. The surface temperature of the nanofluids were recorded by infrared thermal imager, Ray Cam 1886. The stability of the nanofluids over time were observed by a red laser torch.

3. Results and Discussions

3.1 XRD and TEM Analysis

The XRD pattern of f-BNNs is presented in **Fig. 1b** along with that of bulk BN powder. Peaks observed at 2θ values of26.2° and 42.8° were assigned to diffraction originating from (002) and (100) planes of h-BN. From relative intensity ratio it can be concluded that the sample is having (002) preferred orientation agreeing well with JCPDS Card number 340421. The exposed (002) crystal surface of h-BN resembles the (002) plane of graphite [8, 20] -. In case of f-BNNs, presence of no other peak indicated its phase purity. An estimation of the intensity ratio of peaks corresponding to (004) & (100), (I_{004}/I_{100}) plane (inset of **Fig. 1b**) shows a higher ratio for f-BNNs. Hence exfoliation have worked well on (004) plane [23].

The TEM images as shown in **Fig. 2** reveals the morphology**.** It indicates the presence of puckered sheet like structures similar to graphene with an average size approximately of 100-450 nm.

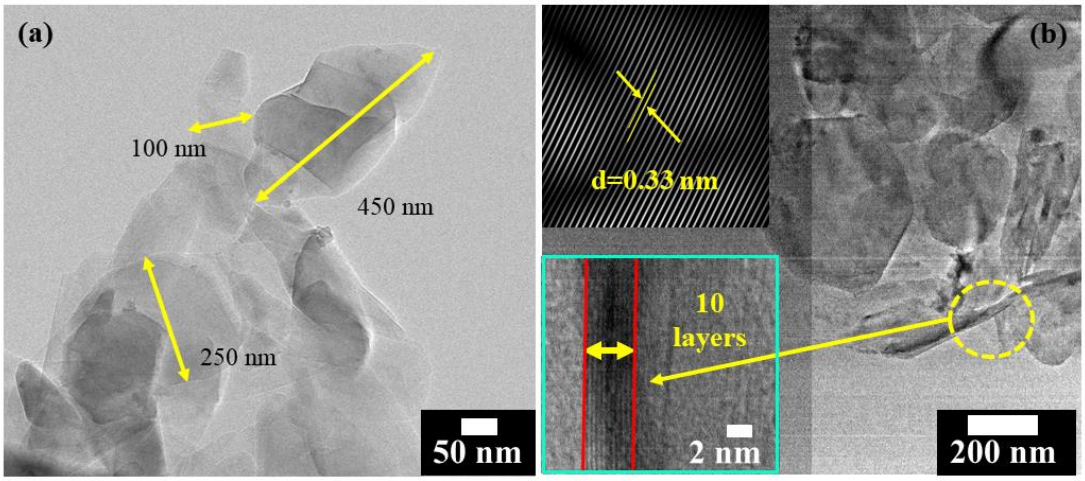

Fig. 2 TEM images of f-BNNs

Further, the crystalline nature of the nanosheets is clearly observed in the lattice imaging (inset, **Fig. 2b**.) obtained by HRTEM. Th*e d* spacing (top inset of **Fig.2b**) as calculated by *Image J* was 0.33 nm, which corresponds to (002) plane of XRD plot. The thickness of the exfoliated sheets were around 5 nm, consisting of 10-12 layers (bottom inset of **Fig. 2b**).

3.2 XPS, RAMAN & FTIR Analysis:

To identify the chemical states of f-BNNs, characterization of f-BNNs by XPS was performed (**Fig. 3)**. The XPS survey plot is depicted in **Fig. 3a w**hereas the high resolution (HR) scan for

B 1s, N 1s, and F 1s are presented in **Fig.3b-3d,** after charge correction considering the C1s peak at 284.6 eV. Oxygen and carbon peaks shown in survey plot most likely resulted from the exposure of f-BNNSs to air or during the XPS measurement groundwork. The detected binding energy of B 1s, N 1s, and F 1s are at 195, 402.4, and 690.33 eV. The measured values are in good agreement with the previous reports [23]. The presence of fluorine is further supported by EDAX analysis provided in the *SI* and FTIR analysis described in the next section.

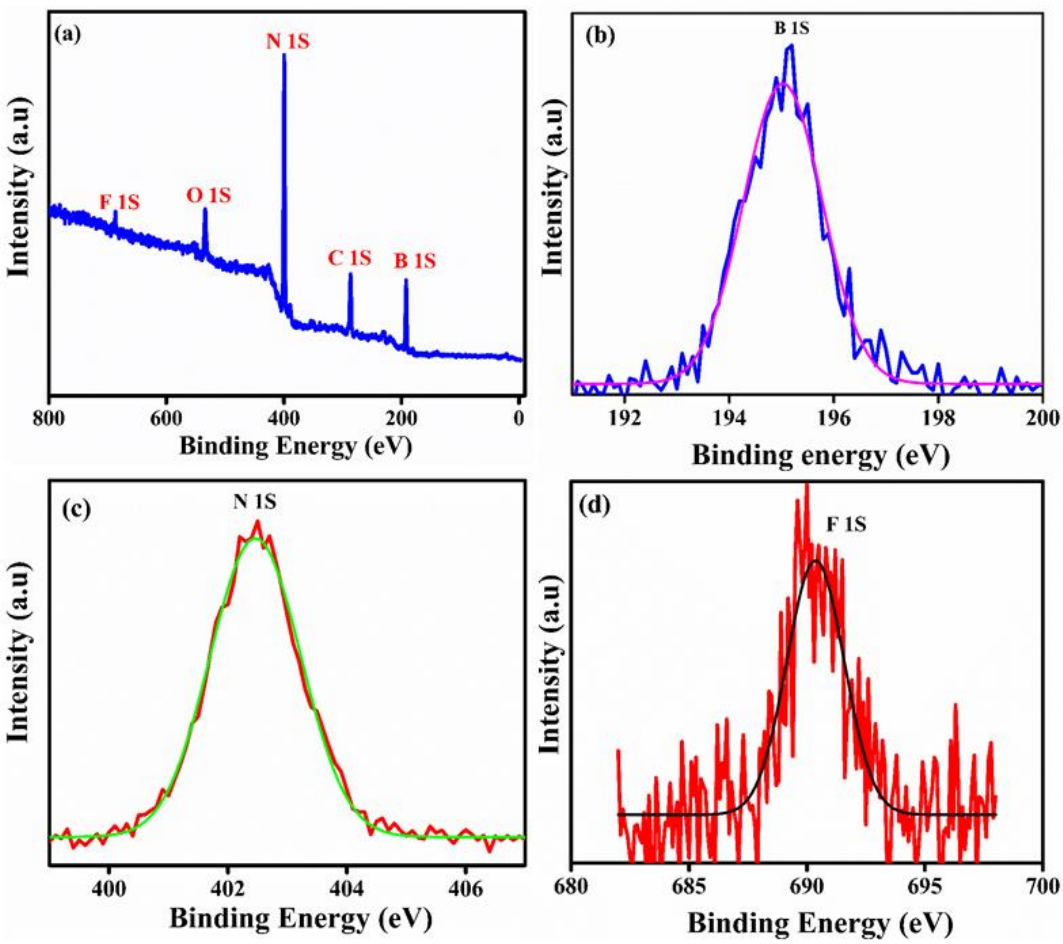

Fig. 3 XPS Analysis of F-BNNs

The RAMAN spectra of the sample as depicted in **Fig.4a.** shows the presence of sharp peak at 1372 cm^{-1}. This peak corresponds to the E_{2g}mode of vibration and appears as a red shift from bulk BN (1374 cm^{-1}) [8]. The red shift occurs due to the exfoliation procedure where number of layer decreases [24]. In FTIR spectra (**Fig. 4b**), two noticeable bands at 814 and 1389 cm^{-1} is noticed which rises due to in-plane stretching and out-of-plane bending vibrations of B-N bond. In addition to these two, an additional broad bond at about 3000 cm^{-1} is observed which indicates B-F bond [24] which proves the bonding of fluorine with Boron. It is also to be noted

that generally a broad -OH bond occurs at around 3000 cm^{-1} due to moisture adsorption on the nanomaterial surface. Hence it is concluded that here, B-F bond and -OH bond have overlapped in this region [24]. This is in line with the results of XPS analysis as discussed in the previous paragraph.

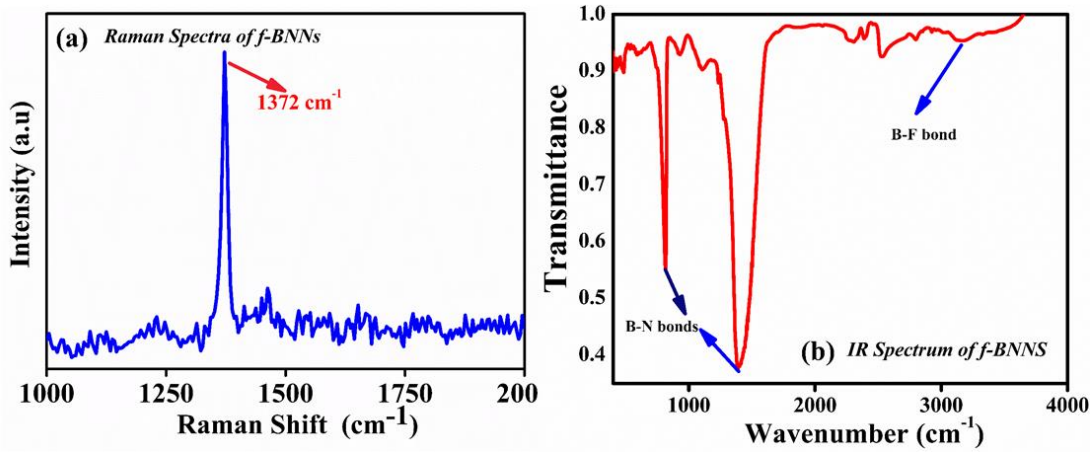

Fig. 4 (a) RAMAN & (b) FTIR Analysis

3.3 Nanofluid preparation

Nanofluids of f-BNNs in transformer oil (TO) were prepared via conventional two-step process [22]. Two different grades of TO similar to our previous work were used as base fluid (BO) [22]. The properties of base fluids are provided briefly in **Table S1** in SI. Nanofluids at three different weight percentages (wt. %), 0.0025, 0.005 & 0.01 in both oils were prepared.

3.4 Impact on Electrical insulation

TO acts as the electrically insulating medium between the high voltage windings. Hence, the impact of the nano-agents on various insulating properties such as, dielectric breakdown (DB) strength, resistivity, dielectric loss, etc. of the liquid insulation system are very important. Following sections evaluate these important electrical properties of the TO nanofluids under study.

3.4.1 AC BDV of Nanofluids

The AC voltage tolerance level of nanofluids were tested on Neo-Teletronix made automatic breakdown voltage tester (120 kV), following IEC 156 standard with a ramp voltage of 2 kV/s using copper electrodes. For all DB measurements conducted here, an average of 18

independent measurements was carried out to calculate the mean BDV. AC BDV depends on various parameters of nanofiller as well as oil [25]. In order to investigate the role of several parameters in monitoring the BD mechanism, different type of measurements was carried out by altering various parameters. This helps to identify and analyse clearly the dominant role played in BDV enhancement and give better clarity of the mechanism. Here, the AC BDV was measured at different experimental conditions such as: (*i) Filler fraction dependent BDV measurement*: For this, spherical copper electrodes (Diameter: 13 nm) at a gap distance of 2.5 mm were kept fixed for both set of nanofluids (**Fig. 5a).** A maximum increase of around 26 % and 20 % in AC BDV for nanofluids with 0.005 & 0.01 wt. % in oil 1 and oil 2 respectively was observable. For oil 1 based nanofluids, detrimental nature in BDV is observed after 0.005 wt. % which was called as optimum concentration.

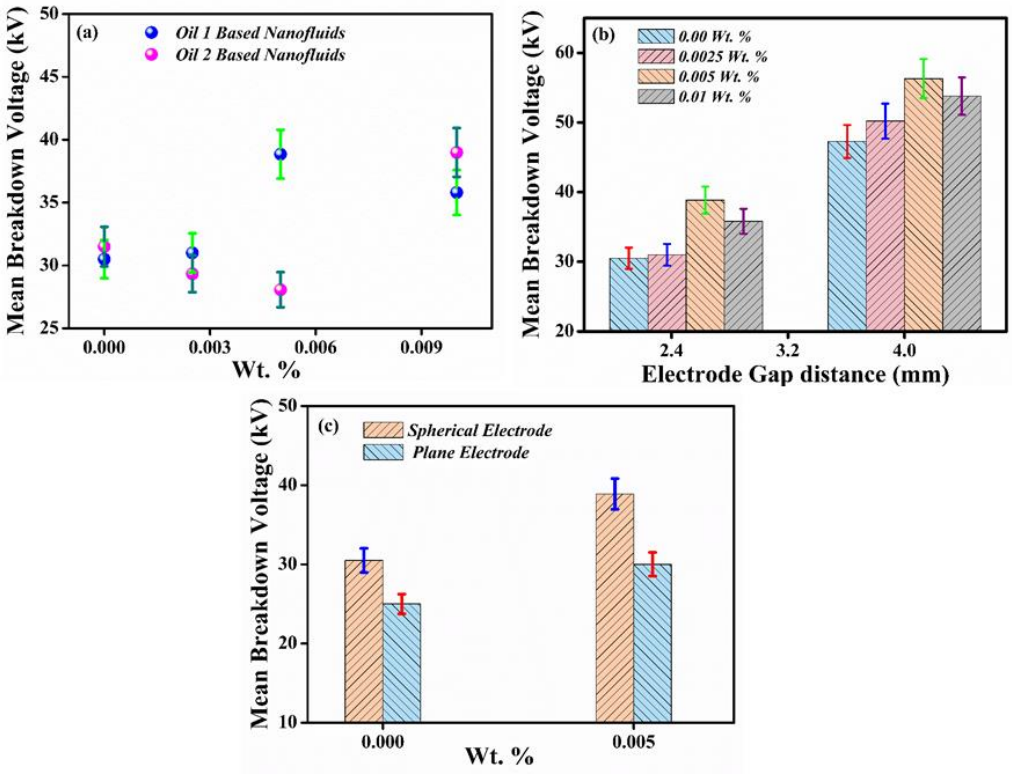

Fig. 5 (a) Filler fraction dependent BDV plot of nanofluids, Variation of BDV with (b) electrode distance & (c) electrode geometry

(ii) Electrode Gap dependent BDV study: For this, the set of oil-1 based nanofluids was chosen and the BDV was measured with spherical copper electrodes with an increased electrode distance of 4 mm (**Fig. 5b**). With increased electrode gap (4 mm), the AC BDV of both the base fluid and nanofluid increases, however the increment in nanofluid was greater by almost 17% *(iii) Electrode Geometry dependent BDV study:* For this, spherical electrodes were

replaced by plane electrodes (gap distance: 2.5 mm, diameter: 30 mm). Optimum concentration of oil-1 based nanofluids, i.e., @ 0.005 wt. % was used for the study here (**Fig. 5c**). With plane electrode configuration, the BDV in both nanofluid and base fluid decreases compared to spherical electrode system but here too, the nanofluid maintained a higher BDV; almost 16 % higher. Hence, either with similar electrode geometry or with similar electrode-gap, nanofluids tolerate more AC voltages than base fluid.

The ability of the utilized nanofillers to enhance BD voltages of transformer oil to a huge extent is explained according to the mostly accepted conjecture behind 'breakdown in insulating fluids'; that is the phenomena of '*Charge trapping*' and the associated *'changing streamer dynamics';* as explained clearly for better clarification below.

The Maxwell-Wagner-Sillar (MWS) theory of polarization for solid-liquid suspensions (such as nanofluids) states that, several surface energy states get induced in the interface of base fluid and nanofiller due to their energy level (*valance, conduction & Fermi, etc*…) differences [25]. The oil-nanofiller interface is a perfect contact; devoid of any abrupt discontinuities in physical features [25] (so that critical theories of grain-boundary or grain resistance is neglected). Now, when the suspension is subjected to high electrical stresses, a copious number of charges (streamer charges) gets injected in the medium. The interfacial states act as sinks of those charges and holds them. The sinks can be of deep or shallow type, depending on the conductivity ($\boldsymbol{\sigma}$) and permittivity (ε) differences of both oil and the nanofiller. A shallow trap can accommodate a streamer charge for a short span and de-trap it easily. While a deep trap stores the charges for a longer time and can create permanent electrets [26]. Presence of these traps and accumulation of charges in the interface states (also known as MWS region [25], trap sites [22]) gives rise to a layer wise charge distribution -surface layer, stern layer & diffuse layer, referred as Electrical double layer (EDL) having thickness in the range of 2 to 9 nm [27]. Due to these charge arrangements in EDLs, the natural streamer orientation and propagation is hindered. A net dipole moment (p) is induced and there is an overall surge in BDV of nanofluid.

The degree of streamer hindrance depends on the density of charge traps [28]. It is generally seen that a conducting nanofiller offer shallow traps with high trap density and can improve BDV at ultralow concentrations [15]. Semi-conducting and insulating materials generally provide shallow to deep trap density at higher filler concentrations [5, 6]. Again, the quantity of charge trapped also depends upon the area of oil-material interface. In this context, choice of appropriate morphology is required [13]. This is where 2D materials prove to be eminent

participators. They voluntarily provide large oil-nanomaterial interface with the largest number of surface-active atoms to participate in a phenomenon among all its morphological brotherhoods. Recalling the role of conducting nanofillers at ultra-low concentrations, choice of 2D nanofiller with a finite conductivity would be a viable approach.

In the current experiment, f-BNNs shows same relative permittivity as of prinstine BN, but a finite conductivity (**Fig. 6a**) is induced due to fluorine incorporation. Hence, the trap type and the BD performance trend are anticipated to be similar to previous studies by BN particles or sheets [7, 8, 20]. Conventional BN nanomaterial under goes polarization and provides traps for streamers under external electric field [7, 8]. What provides additional attention here is the role of *2D morphology* and *incorporated fluorine* as explained below. (While discussing, it is assumed that the other parameters that monitors the insulation of the medium such as purity, moisture content, and acidity are unaltered in this experiment).

(i) The specific surface area (SSA) of the interfacial zone or the potential barrier region (oil-nanofiller interface) is proportional to the aspect ratio of the nanofiller. The quantity of trapped charges depends on this SSA. This defends the usage of 2D nanofiller as it will help to trap more charges than other morphologies such as spherical/ cylindrical/ micro particles at the same concentrations. I.e, the spatial distribution of traps increases with the rise in SSA of the barrier.

(ii) Fluorine is highly electro-negative in nature. The introduction of fluorine has helped to induce a finite (though small) conductivity (**Fig.S2**) via decrease of band gap (Kubelka Munk plot, **Fig.S3**). The change in bandgap indicates there is induction of extrinsic energy bands between the valence and conduction bands (VB & CB) of f-BNNs. Hence, the oil-nanofiller interface will be enriched with more trap centres than that of pristine BN (**Fig. 6a**). Which implies higher electro-negativity of f-BNNs than pristine BN. Though a precise determination of electronegativity (via surface charge measurements techniques) are not easily accessible for oil-based solutions, an estimation of the resultant electro-negativity can be done by taking the mean of electro-negativities of the constituent elements of a compound [29]. Therefore, there is trapping of copious charges in the Layers of EDL of f-BNNs-TO nanofluid. An electron from oil is captured in VB as well as other extrinsic states (near VB) of f-BNNs (**Fig. 6a**). This brings a –ve charge accumulation in layer 1 (surface layer) with increased density of charges. The next layer (stern layer); layer of counter-particles (+ve) has a gradient of decreasing intensity from the material towards the oil. Due to high charge density of surface layer, stern and diffuse

layer will also contain more charges (**Fig. 6b**). Hence, the temporal distribution of traps increases with the induction of fluorine in pristine BN. As a result, more BDS is observed at lower filler fraction compared to BN sheets / particles (**Fig. 7a**).

The spatio-temporal charge accumulation with time continues in a manner analogous to capacitor charging phenomena and prevents the streamers to bridge the electrodes. However, the process cannot continue for infinite time as there would be a saturation. The dispersed nanosheets gets charge saturated and can't accommodate incoming charges further. The migration of charges to CB via hopping takes place through the induced states as shown schematically in **Fig. 6a.** This leads to transient generation of Schottky current and breakdown [26].

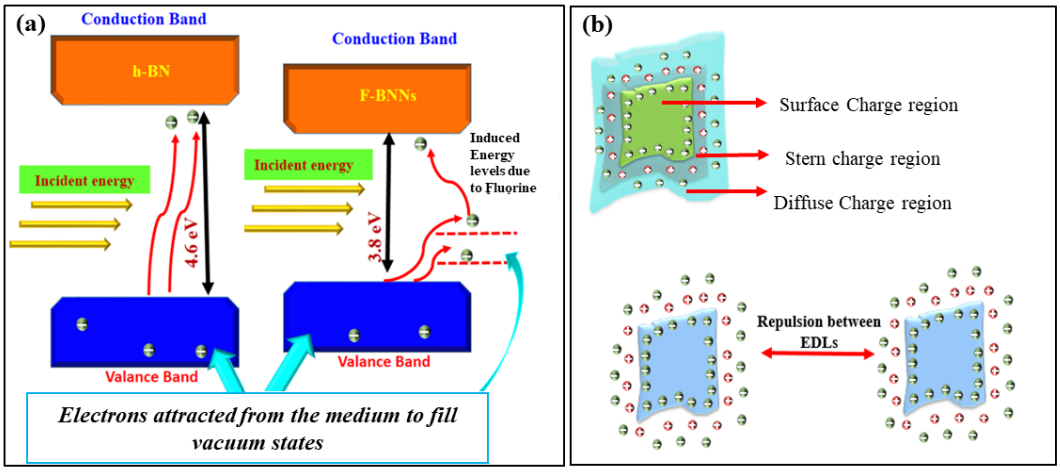

Fig. 6 (a) Trapping of streamer charges in pristine BN and f-BNNs & (b) EDL arrangement in f-BNNs/oil interface

With increasing wt. %, the number of traps increases resulting in further increase of BDV (**Fig. 5a**). But, after a critical concentration, (here 0.005 wt. % in oil 1), the inter-sheet distance in the medium decreases which causes an overlap of the interfacial zones /EDL regions of two or more sheets. This causes hindrance in electrostatic stabilization and upsurges Van der Waals forces and creates a scattering-free and resistance free escape of streamers through the EDL region [22]. The apparent time required to trap a free charge becomes larger than the time required for a free charge to traverse the gap. Hence accumulation of carriers occurs resulting in numerous arc-discharges and ultimately the oil become conducting.

Further, the augmentation in BDV in oil 1 based nanofluids are higher than that observed in oil 2 based nanofluids. This is due to the fact of oil 2 possessing 10 times lower resistivity than oil 1. Hence oil 2 intrinsically have low tolerance level to electrical shocks. This requires a large

number of nanosheets in oil 2 to enhance the electrical BDV to the level of oil-1 based nanofluids. With increasing electrode distance, the distance to be travelled by the streamers to cause breakdown increases. Hence a delay in streamer propagation is reflected in the higher BDV with increased electrode distance (**Fig. 5b**). The dependency of BDV on electrode geometry is explained on the context of the differences of electric field intensity between the electrodes. With spherical electrode configuration, the streamers orientation is divergent while with plane electrode configuration, a linear orientation of streamer is obvious between the electrodes [30]. Hence the field intensity in the former case is smaller than the latter. Which implies that the probability of trapping streamer charges will be higher for spherical electrode system. With plane electrode system, due to high density of lines of force, streamers would successfully short the electrode at relatively shorter time. This explains the results obtained with electrode variation conditions (**Fig. 5c**).

Finally, a comparative experimental study was carried out to support the claims made. For this, BD study with bulk BN, exfoliated BN and f-BNNs at 0.005 wt. % (**Fig. 7a**) was carried out. From the relative performances, it is concluded that, the currently developed material is the most reliable one among the rising opponent in the field of liquid insulation.

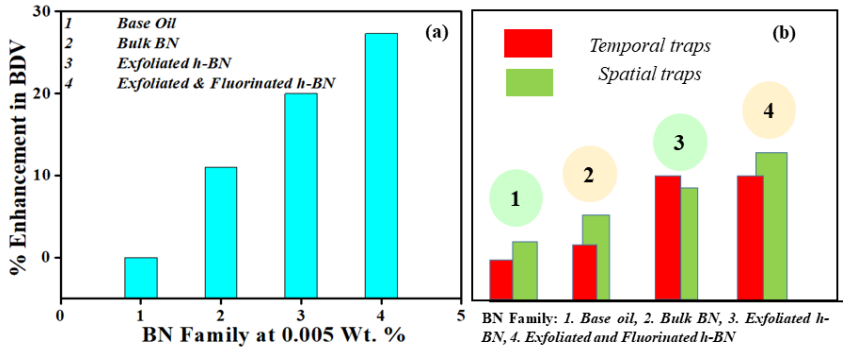

Fig. 7 Comparative BDV Study of BN family

3.4.2 Resistivity, Relative permittivity and Dielectric Loss Analysis:

These are some other electrical properties, necessary to assess the quality of oil. It is well known that every dielectric consists of capacitive and resistive component. The capacitive component gives idea about the ability of the dielectric to store charges whereas the resistive component gives idea about how the dielectric allows the flow of current through it. The loss tangent describes the resistive to capacitive loss. Under AC voltage, the ability of the dielectric to bound charges is defined by relative permittivity [9]. Under DC voltage, the ability of the dielectric to block the flow of current is defined by resistivity [9]. All these are essential to check the quality of the oil. These measurements were done using ADTR 2K PLUS instrument

for both set of nanofluids at four different temperatures (45, 60, 75, 90°C). The results are plotted in **Fig. 8a-8c** below.

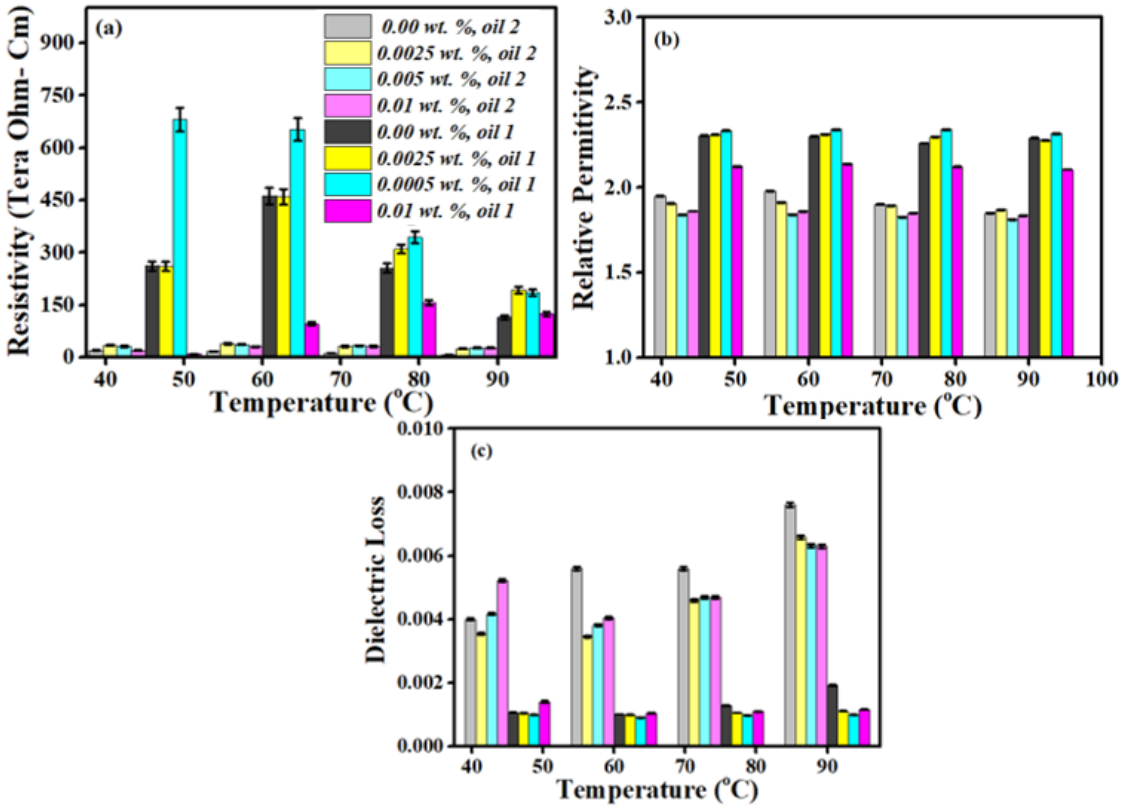

Fig. 8 (a) Resistivity, (b) Relative permittivity & (c) Dielectric Loss of nanofluids in two different oils

Fig. 8a depicts the variation of resistivity of nanofluids in two different base fluids. In both cases, nanofluids (upto certain concentration) exhibits higher resistivity than base fluids. With the increase in temperature, the resistivity falls due to increase in thermal agitation. These results are consistent with AC breakdown results. The variation in relative permittivity (ε) as depicted in **Fig. 8b** shows that there is a rise in ε value for nanofluids in oil 1, compared to oil 2. The dielectric loss is seen to decrease in nanofluids in both oils (**Fig. 8c).** It is interesting to note that loss at higher temperature is more for base oil, with nanofluids, a drastic drop in loss is observed.

The reason for the variation of all three properties described above is due to the similar phenomena of charge trapping in extrinsic energy states as discussed in the AC BDV section. Also, the loss in oil 2 is higher than oil 1 due to the resistivity differences between the two original oil.

3.5 Impact on Thermo-physical Properties

3.5.1 Thermal conductivity, Thermal response & Thermal Images

The temperature dependent thermal conductivities (*k*) of base fluid and nanofluids (in oil 1) were measured and represented in **Fig. 9a**. There exists a linear relationship between thermal conductivity and wt. % &temperature. A maximum enhancement of ~8% in *k* is obtained for 0.01 wt. % nanofluid at 50° C. The results follow the trend predicted by Maxwell [20] and remain within limits predicted by HC hypothesis [31]. Further, to support the results, thermal response characteristics (heating and cooling) and infrared (IR) images during different instances of heating and cooling of base oil and nanofluid (0.01 wt. %) were recorded under same physical conditions; as presented in **Fig. 9b-Fig.9d** respectively.

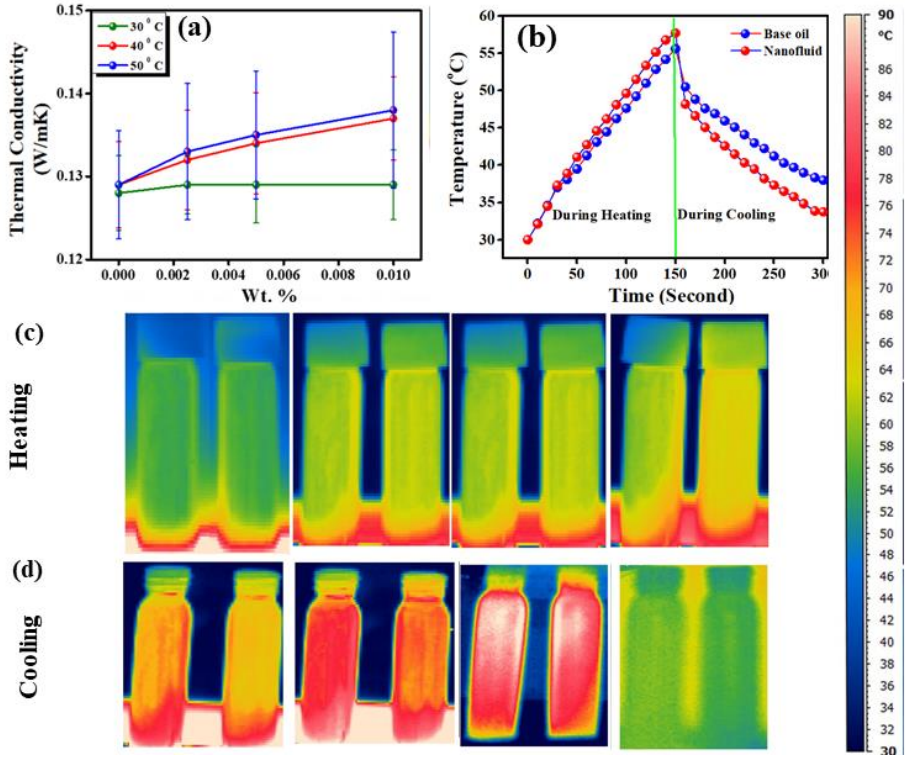

Fig. 9 (a) Temperature dependent Thermal conductivity, (b) Thermal characteristics & (c) Infrared Images of the base fluid (left) and nanofluid (0.01 wt. %, right) during heating and cooling

It follows that the nanofluid gets heated faster than the base fluid as well as cool down easily; i.e the specific heat decreases in nanofluids. Analysing the IR images from the IR temperature scale, it follows that the temperature profile is higher in every interval of heating in nanofluid.

During cooling, the nanofluid gets cooled much easily. Hence nanofluids endure more heat dissipation capability than base oil.

The rise in thermal conductivity is attributed to the rise in the rate of phonon transport in the medium. For nano-suspensions, the molecular liquid layering at the interface acts as the bridge of ballistic heat transfer. The nature (smoothness) of the interface is hence of immense importance. In this experiment, 2D f-BNNs, owing to its higher aspect ratio, thinness (5nm, 10-12 layers) and lipophilic nature provides a large smooth interface; which enables restriction free propagation of acoustic phonons facing low Kapitza resistance [32]. With rising temperature, the molecules in the nanostructures tremble about their mean site and the contribution of Brownian motion in heat transfer gains merit [33]. Apart from the morphology, hexagonal phase of the dispersed material has played its role in providing consent to long range phonon transfer along the c-axis of hexagonal unit cell [8, 20].

3.5.2 Stability

The most important factor that decides the industrial applicability of a nanofluid is its stability. The stability of the nanofluid was checked by Tyndall scattering (room temperature) as shown in **Fig. 10**. It is seen that nanofluid is stable after one month of preparation.

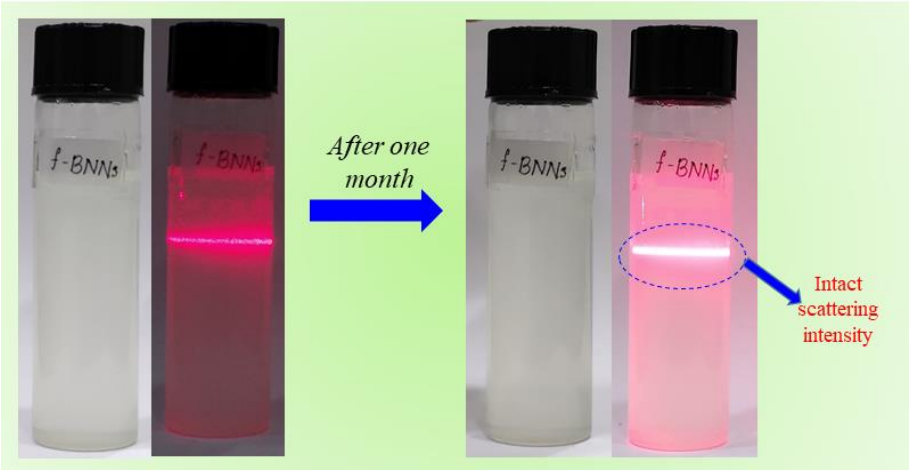

Fig. 10 Tyndall scattering image of nanofluid (0.01 wt. %) after just preparation & after 1 month of preparation.

The reason for the stability is embedded in the physics of fluorine incorporation. It is well known that the electro-static repulsion between nanofiller defends the stability against the attractive van der Waals forces among the nanofillers in nanofluids [34]. Inoculation in BN by highly electro-negative fluorine and the comparatively low wt. % of the nanofluid provided natural electrostatic repulsion (**Fig. 6d**) and helped to stabilize the medium. The nanofluid was seen to be resistant against gravity for a couple of months without any agglomeration. Hence,

it is obvious that in real time operating conditions in electrical transformers, it will provide great solutions in reducing the burden of modern power system challenges**.**

Finally, a comparative table showing the relative performance of all BN based materialsin transformer oil were surveyed and presented in **Table 1**.

Table 1. Comparative Table

Morphology, Size (nm) & Base Fluid	**AC BDV increment (%)**	**Other Electrical Properties**	**Stability**	**Reference**
Nanosphere, 50 nm, Transformer oil	11 % (@ 0.05 wt. %)	Improved Resistivity, DC BDV, relative permittivity & dielectric Loss	Not studied	[7]
Nanosheets, 100-450 nm, Transformer Oil	-	-	3 months	[8]
h-BN Nanosheets, Cottonseed oil	12 % (@0.01 Wt. %)	Improved impulse BDV & resistivity, reduced dielectric loss	Stable (studied for a week)	[9]
h-BN Nanosheets, few layers, Mineral Oil	-	Improved resistivity & reduced dielectric loss	Surfactant-free Ultra-stable	[21]
BN nanoparticles. 50 nm, Vegetable oil	-	Improved resistivity, relative permittivity & trap characteristic, reduced dielectric loss & electrical conductivity	Not studied	[35], year
Present work: f-BN nanosheets (100-450nm, 5 nm thickness)	20-26 % (@0.01 -0.005 wt %	Improved resistivity, relative permittivity & reduced dielectric loss	Ultra-stable for several months	-

4. Conclusions:

A simple chemical method of fluorination is adopted here for improvement of twin goals of TO NFs – AC Breakdown Voltage and long-term stability. The attachment of a small quantity of conductive fluorine on highly insulating h-BN nanosheets has played a vital role in reducing the band gap. It offered plenty of charge trapping sites and resulted in huge surge of AC BDV as compared to the state-of-the-art BN family. Whereas the lipophilic nature, 2D morphology

and high electronegativity enabled electrostatic repulsion among the EDLs of the nanosheets provided long term stability of the nanofluid without usage of any long chain surfactant. This path breaking idea opens a new horizon in designing future tailor made functionalised nanofillers for next generation NFs to meet the multiple objectives.

Declaration of competing interest

The authors declare that they have no known competing financial interests or personal relationships that could have appeared to influence the work reported in this paper.

Authorship contribution statement

Mississippi M. Bhunia: Conduction of experiments (synthesis & application part), analysis & plotting of results, drafting, synchronizing, editing, images formatting.**Kalyan Kumar Chattopadhyay & Paramita Chattopadhyay:**Idea behind the work, Material selection, discussions and manuscript correction.

ACKNOWLEDGEMENTS:

Authors gratefully acknowledge the financial support provided by Central Power Research Institute, Ministry of power, GOI. Help rendered from Jadavpur University and IIEST Shibpur for instrumental support are gratefully acknowledged. Mississippi is indebted to IIEST Shibpur for her fellowship. Karamjyoti Panigrahi is thanked for the purpose of manuscript editing and suggesting the arrangement of the content.

References

1. S. U Choi, J. A. Eastman, Enhancing thermal conductivity of fluids with nanoparticles: Argonne Nat. Lab. IL (United States), CONF-951135-29 (1995) ANL/MSD/CP-84938
2. M.U. Sajid, H.M. Ali, Recent advances in application of nanofluids in heat transfer devices: a critical review, Renew. Sustain. Energy Rev. 103 (2019) 556-592. https://doi.org/10.1016/j.rser.2018.12.057
3. V. Segal, A. Hjortsberg, A. Rabinovich, D. Nattrass, K. Raj, AC (60 Hz) and impulse breakdown strength of a colloidal fluid based on transformer oil and magnetite nanoparticles: In Conference Record of the 1998 IEEE International Symposium on Electrical Insulation (Cat. No. 98CH36239) 2 (1998) 619-622

4. Y. Lv, Q. Du, L. Wang, Q. Sun, M. Huang, C. Li, B. Qi, Effect of TiO_2 nanoparticles on the ion mobilities in transformer oil-based nanofluid, AIP Advances, 7(10) (2017) 105022. https://doi.org/10.1063/1.4999260
5. U.Khaled, A. Beroual, DC breakdown voltage of natural ester oil-based Fe_3O_4, Al_2O_3, and SiO_2 nanofluids: Alex. Eng. J. 56 (6), (2020) 4611-4620. https://doi.org/10.1016/j.aej.2020.08.016
6. M. Rafiq, L. Chengrong, Y. Lv, Effect of Al_2O_3 nanorods on dielectric strength of aged transformer oil/paper insulation system: J. of Mol. Liq. 284 (2019) 700-708. https://doi.org/10.1016/j.molliq.2019.04.041
7. B. X. Du, X. L. Li, J. Li, Thermal conductivity and dielectric characteristics of transformer oil filled with BN and Fe_3O_4 nanoparticles: IEEE Trans. Dielectr. Electr. Insul. 22(5) (2015) 2530-2536. 10.1109/TDEI.2015.005079
8. M. M. Bhunia, S. Das, P. Chattopadhyay, S. Das, K.K. Chattopadhyay, Enhancement of thermal conductivity of transformer oil by exfoliated white graphene nanosheets: IEEE 16th International Conference on Environment and Electrical Engineering (EEEIC) (2016) 1-5
9. R.A. Farade, N.I.B.A. Wahab, D.E.A. Mansour, N.B. Azis, J. Jasni, N.R. Banapurmath, M.E.M., Soudagar, Investigation of the dielectric and thermal properties of non-edible cottonseed oil by infusing h-BN nanoparticles: IEEE Access, 8 (2020) 76204-76217. 10.1109/ACCESS.2020.2989356
10. Hao, J., Dan, M., Liao, R. and Li, J., 2019. Effect of moisture on particles accumulation and oil breakdown characteristics in mineral oil and natural ester under non-uniform DC electrical field. IEEE Access, 7, pp.101785-101794. 10.1109/ACCESS.2019.2930574
11. J. Fal, O. Mahian, G. Żyła, Nanofluids in the Service of High Voltage Transformers: Breakdown Properties of Transformer Oils with Nanoparticles, a Review: Energies 11(11) (2018) 2942. 10.3390/en11112942
12. X. Wang, Z. D. Wang, Particle effect on breakdown voltage of mineral and ester-based transformer oils: In Annual Report Conference on Electrical Insulation and Dielectric Phenomena (2008) 598-602
13. M.S. Mohamad, H. Zainuddin, S. Ab Ghani, I.S. Chairul, AC breakdown voltage and viscosity of palm fatty acid ester (PFAE) oil-based nanofluids: J. Electr. Eng. Technol. 12(6) (2017) 2333-2341. https://doi.org/10.5370/JEET.2017.12.6.2333

14. W. Sima, J. Shi, Q. Yang, S. Huang, X. Cao, Effects of conductivity and permittivity of nanoparticle on transformer oil insulation performance: Experiment and theory. IEEE Trans Dielectr Electr Insul. 22(1) (2015) 380-390. 10.1109/TDEI.2014.004277

15. P. Dhar, A. Katiyar, L.S. Maganti, A. Pattamatta, S.K. Das, Superior dielectric breakdown strength of graphene and carbon nanotube infused nano-oils: IEEE Trans Dielectr Electr Insul. 23(2) (2016) 943-956. 10.1109/TDEI.2015.005477

16. Y. Hou, Z. Zhang, J. Zhang, Z. Wang, H. Liu, Experimental investigations into the enhanced dielectric breakdown performances of propylene carbonate modified by TiO_2 nanoparticles: IEEE Trans Dielectr Electr Insul. 23(5) (2016) 2816-2821. 10.1109/TDEI.2016.7736841

17. Y. Lv, Y. Ge, Z. Sun, Q. Sun, M. Huang, C. Li, B. Qi, J. Yuan, Z. Xing, Effect of nanoparticle morphology on pre-breakdown and breakdown properties of insulating oil-based nanofluids. Nanomaterials 8(7) (2018) 476 https://doi.org/10.3390/nano8070476

18. Y. Hou, Z. Zhang, J. Zhang, Z. Liu, Z. Song, Effect of $BaTiO_3$ nano-particles on breakdown performance of propylene carbonate. Rev. Sci. Instrum. 86(5), (2015) 054702. https://doi.org/10.1063/1.4920997

19. P.K. Das, N. Islam, A.K. Santra, R. Ganguly, Experimental investigation of thermophysical properties of Al_2O_3–water nanofluid: Role of surfactants: J. of Mol. Liq. 237 (2017) 304-312. https://doi.org/10.1016/j.molliq.2017.04.099

20. H. Xiao, S. Liu, 2D nanomaterials as lubricant additive: A review: Mat. & Des. 135 (2017) 319-332. https://doi.org/10.1016/j.matdes.2017.09.029

21. J. Taha-Tijerina, T.N. Narayanan, G. Gao, M. Rohde, D.A. Tsentalovich, M. Pasquali, P.M Ajayan, Electrically insulating thermal nano-oils using 2D fillers: Acs Nano, 6(2) (2012) 1214-1220. https://doi.org/10.1021/nn203862p

22. M.M. Bhunia, M.M., K. Panigrahi, C. B. Naskar, S. Bhattacharjee, K.K. Chattopadhyay, P. Chattopadhyay, 2D square nanosheets of Anatase TiO_2: A surfactant free nanofiller for transformer oil nanofluids: J. of Mol. Liq. 325 (2021) 115000. https://doi.org/10.1016/j.molliq.2020.115000

23.. Y. Xue, Q. Liu, G. He, K. Xu, L. Jiang, X. Hu, J. Hu, Excellent Electrical Conductivity of the Exfoliated and Fluorinated Hexagonal Boron Nitride nanosheets: Nanoscale research letters, 8(1) (2013) 1-7. https://doi.org/10.1186/1556-276X-8-49

24. M. Du, X. Li, A. Wang, Y. Wu, X. Hao, M. Zhao, One-step exfoliation and fluorination of boron nitride nanosheets and a study of their magnetic properties: Angewandte Chemie International Edition, 53(14) (2014) 3645-3649. https://doi.org/10.1002/anie.201308294

25. K. Wu, C. Cheng, Interface charges between insulating materials, IEEE Trans Dielectr Electr Insul. 24 (2017) 2633-2642. 10.1109/TDEI.2017.006442

26. S.K. Garg, Dielectric Relaxation processes and charge transport mechanism in Liquid crystalline copolyesteramide Vectra B950 polymer: NIT Kurukshetra (2018).

27. Y. Peng, Z. Tong, Y. Yang, C.Q. Sun, The common and intrinsic skin electric-double-layer (EDL) and its bonding characteristics of nanostructures: Appl. Surf. Sci. 539(2021), 148208. https://doi.org/10.1016/j.apsusc.2020.148208

28. Y. Du, Y. Lv, C. Li, M. Chen, J. Zhou, X. Li, Y. Zhou, Y. Tu, Effect of electron shallow trap on breakdown performance of transformer oil-based nanofluids: J. Appl. Phys. 110(10) (2011) 104104. https://doi.org/10.1063/1.3660783

29. D.E.A. Mansour, A.M. Elsaeed, M. A. Izzularab, The role of interfacial zone in dielectric properties of transformer oil-based nanofluids: IEEE Trans Dielectr Electr Insul. 23(6) (2016) 3364-3372. 10.1109/TDEI.2016.005697

30. J.W. Wang, M.H. Wang, L. S. Jang, Effects of electrode geometry and cell location on single-cell impedance measurement: Biosens. Bioelectron. 25(6) (2010) 1271-1276. https://doi.org/10.1016/j.bios.2009.10.015

31. S. Bhanushali, N.N. Jason, P. Ghosh, A. Ganesh, G.P. Simon, W. Cheng, Enhanced Thermal Conductivity of Copper Nanofluids: The Effect of Filler Geometry, ACS Appl. Mater Inter. 9 (2017) 18925-18935. https://doi.org/10.1021/acsami.7b03339

32. A. Khodayari, M. Fasano, M. B. Bigdeli, S. Mohammadnejad, E. Chiavazzo, P. Asinari, Effect of interfacial thermal resistance and nanolayer on estimates of effective thermal conductivity of nanofluids:Case Stud. Therm. Eng. 12 (2018) 454-461. https://doi.org/10.1016/j.csite.2018.06.005

33. N. De-Ming, W. Chang-Bin, Direct numerical simulation of particle Brownian motion in a fluid with inhomogeneous temperature field: Thermal Science, 24(6A) (2020) 3707. https://doi.org/10.2298/TSCI180612098N

34. T. Cao, M. Elimelech, Colloidal stability of cellulose nanocrystals in aqueous solutions containing monovalent, divalent, and trivalent inorganic salts: J. Colloid Interface Sci. 584 (2021) 456-463. https://doi.org/10.1016/j.jcis.2020.09.117

35. B.X. Du, X. L. Li, Dielectric and thermal characteristics of vegetable oil filled with BN nanoparticles: IEEE Trans Dielectr Electr Insul. 24(2) (2017) 956-963.10.1109/TDEI.2017.005758